JACS
JOURNAL OF THE AMERICAN CHEMICAL SOCIETY

Article

Cite This: J. Am. Chem. Soc. 2018, 140, 6718−6726

pubs.acs.org/JACS

Elucidation of the Formation Mechanisms of the Octahydrotriborate Anion ($B_3H_8^-$) through the Nucleophilicity of the B−H Bond

Xi-Meng Chen,[†,⊥] Nana Ma,[†,⊥] Qian-Fan Zhang,[‡] Jin Wang,[†] Xiaoge Feng,[†] Changgeng Wei,[†] Lai-Sheng Wang,[*,‡] Jie Zhang,[*,†] and Xuenian Chen[*,†]

[†]School of Chemistry and Chemical Engineering, Henan Key Laboratory of Boron Chemistry and Advanced Energy Materials, Henan Normal University, Xinxiang, Henan 453007, China

[‡]Department of Chemistry, Brown University, Providence, Rhode Island 02912, United States

Supporting Information

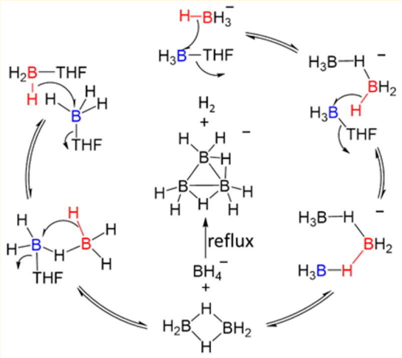

ABSTRACT: Boron compounds are well-known electrophiles. Much less known are their nucleophilic properties. By recognition of the nucleophilicity of the B−H bond, the formation mechanism of octahydrotriborate ($B_3H_8^-$) was elucidated on the bases of both experimental and computational investigations. Two possible routes from the reaction of BH_4^- and THF·BH_3 to $B_3H_8^-$ were proposed, both involving the B_2H_6 and BH_4^- intermediates. The two pathways consist of a set of complicated intermediates, which can convert to each other reversibly at room temperature and can be represented by a reaction circle. Only under reflux can the B_2H_6 and BH_4^- intermediates be converted to $B_2H_5^-$ and $BH_3(H_2)$ via a high energy barrier, from which H_2 elimination occurs to yield the $B_3H_8^-$ final product. The formation of B_2H_6 from THF·BH_3 by nucleophilic substitution of the B−H bond was captured and identified, and the reaction of B_2H_6 with BH_4^- to produce $B_3H_8^-$ was confirmed experimentally. On the bases of the formation mechanisms of $B_3H_8^-$, we have developed a facile synthetic method for MB_3H_8 (M = Li and Na) in high yields by directly reacting the corresponding MBH_4 salts with THF·BH_3. In the new synthetic method for MB_3H_8, no electron carriers are needed, allowing convenient preparation of MB_3H_8 in large scales and paving the way for their wide applications.

INTRODUCTION

The octahydrotriborate anion, as a basic hydroborate unit following BH_4^- and $B_2H_7^-$, plays important roles in boron chemistry.[1,2] The preparation of the alkali salts of octahydrotriborate dated back to Stock's work in the 1920s.[2a] By shaking potassium or sodium amalgam in the presence of diborane gas, a new compound with an empirical formula of $K(B_2H_6)$ or $Na(B_2H_6)$ was obtained.[2a−c] In 1949, Newkirk found that the compound with the empirical composition of $Na(B_2H_6)$ had an identical X-ray powder diffraction pattern to sodium borohydride ($NaBH_4$),[3] the structure of which was first characterized by X-ray powder diffraction in 1947.[4] The products of the reaction between sodium amalgam and diborane were finally determined to be a mixture of NaB_3H_8 and $NaBH_4$ in 1:1 ratio based on the results of X-ray, infrared, and elemental chemical analyses in the late 1950s.[5] Since then, the preparation methods for octahydrotriborate salts have been continually improved,[2a−j] but its formation mechanisms have not been fully understood.[1a,2k−o] Recently, the bonding in the $B_3H_8^-$ anion has also been analyzed, highlighting its high stability.[6]

The incremental improvement of the synthetic methods for octahydrotriborate[2a−j] has been mainly focused on using other boranes to replace the flammable and toxic diborane[2d−i] or dispersing sodium on other media (eq 1), instead of using sodium amalgam, which causes health and safety concerns.[2e,f]

$$2\,M/(\mathrm{media}) + 4\,THF{\cdot}BH_3 = MB_3H_8 + MBH_4 + 4\,THF$$
$$M = \text{alkili metals} \tag{1}$$

Potassium, rubidium, and cesium salts of $B_3H_8^-$ were also prepared by the reactions of THF·BH_3 with the corresponding alkali metal amalgams.[2d] Very recently, K/Na alloy was successfully used to prepare the potassium salt of $B_3H_8^-$.[2i] Here we report an investigation on the formation mechanisms of $B_3H_8^-$ upon recognition of the importance of the B−H bond nucleophilic properties, leading to a more convenient preparative method for LiB_3H_8 and NaB_3H_8 by simply using the more convinient MBH_4 compounds (eq 2):

$$MBH_4 + 2\,THF{\cdot}BH_3 = MB_3H_8 + H_2 + 2\,THF$$
$$M = \text{Li and Na} \tag{2}$$

Boron and boron-containing compounds are characterized by their electron deficiency so that BH_3 or BR_3 groups usually act as Lewis acids in reactions with Lewis bases to form Lewis acid−base adducts.[7] Hydroborations are well-known for borane complexes.[8] In this class of reactions, it is generally understood that the electron-deficient boron uses its empty 2p orbital to

Received: April 8, 2018
Published: May 7, 2018

DOI: 10.1021/jacs.8b03785

Scheme 1. Hydroboration Reactions of Borane Complexes (A) and Nucleophilic Substitution Reactions of Borane Complexes (B)

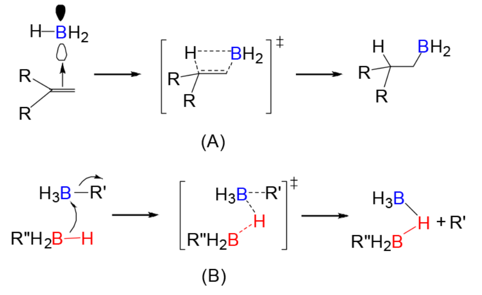

(R = alkyl; R' = THF, $(CH_3)_2S$; R'' = H^-, NH_2^-, THF, and NH_3)

interact with the electron-rich C═C, C═O, C═N double bonds or C≡C triple bond of substrates, leading to an addition reaction of the B–H bond (Scheme 1A).[9] On the other hand, the slightly lower electronegativity of boron (2.0 in the Pauling scale) compared to that of hydrogen (2.1) makes the hydrogen atoms on boron slightly negative in boron hydrides ($B^{\delta+}$–$H^{\delta-}$). Thus, the partially negatively charged hydrogen atoms in boron hydrides possess Lewis base properties. This Lewis base property of the B–H bond enables $R''BH_3$ (R'' = H^-, NH_2^-, THF, and NH_3) to be a nucleophilic reagent in nucleophilic substitution reactions as shown in Scheme 1B. Even though the Lewis acid property of boron complexes has been well recognized,[7f,10] relatively little is known about the Lewis base property of the B–H bond.

In a few known examples of nucleophilic substitution reactions involving the B–H bond as a nucleophilic reagent (red in Scheme 1B), the hydride on the B–H bond usually attacks another boron atom (blue) to form an unsupported B–H–B 3c–2e bond. In fact, the dimerization of two BH_3 groups to form diborane belongs to this type of reactions (Scheme S1a). With this important property of the B–H bond, new boron chemistry has been developed recently.[11a−d] For example, the hydride of the B–H bond in ammonia borane (NH_3BH_3, AB) has been used to substitute THF in THF·BH_3 to form ammonia diborane ($NH_3BH_2(\mu\text{-}H)BH_3$, AaDB), which is unstable but can be observed in ^{11}B NMR.[11a] The observation of this intermediate involving the unsupported B–H–B bond is critical for understanding the formation mechanism of the diammoniate of diborane ($[H_2B(NH_3)_2][BH_4]$, DADB), which has puzzled chemists for many years.[11a,d−i] Furthermore, by use of the same nucleophilic substitution of NH_3BH_3 and THF·BH_3, a facile preparative method for aminodiborane ($NH_2B_2H_5$, ADB) has been developed.[11b,c] From this point of view, the borohydrate (BH_4^-) and its organic borohydrate derivatives ($BH_2R_2^-$) can also be considered as a nucleophilic reagent and their reactions with transition metal or lanthanide cations to form single, double, or triple M–H–B bonds should belong to the nucleophilic substitution reactions.[12]

■ RESULTS AND DISCUSSION

Nucleophilic Behaviors of the B–H Bond. According to the Lewis base property of the B–H bond, four-coordinated $R''BH_3$ complexes (R'' = H^-, NH_2^-, THF, and NH_3) can act as a nucleophile using its B–H bond to substitute a weaker base from a Lewis acid–base adduct. The role of the bonding pair electrons in the B–H bond in this reaction is similar to that of the lone pair electrons in classical nucleophiles. For example, both the lone pair electrons and the B–H bond in the $NH_2BH_3^-$ anion can act as a nucleophile leading to nucleophilic substitution reactions, but the products are different. When $NaNH_2BH_3$ reacted with AB, the lone pair electrons on N attacked the B atom in AB to form $Na[NH_2(BH_3)_2]$ with one NH_3 leaving (Figure S1 and Scheme 2A).[13] In contrast, when $NaNH_2BH_3$ reacted with THF·BH_3, the final products are $(NH_2BH_2)_n$ polymer and BH_4^-.[14] It is believed that in this reaction the B–H bond in the $NH_2BH_3^-$ anion acts as a nucleophile to attack the B atom in THF·BH_3 to form $NH_2BH_2(\mu\text{-}H)BH_3^-$ first and then convert to $(NH_2BH_2)_n$ polymer and BH_4^- with the bridge hydrogen moving to the BH_3 moiety in the unsupported B–H–B bond (Scheme 2B).

Scheme 2. Reactions of $NaNH_2BH_3$ with AB (A) or THF·BH_3 (B)

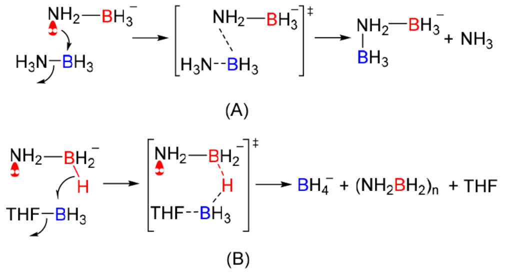

Stability of the Unsupported B–H–B Bond. The newly formed unsupported B–H–B bond by the B–H bond nucleophilic substitution is unstable and can easily cleave. The unsupported B–H–B bond only occurs in weak or noncoordinating solvents or when it is stabilized by additional chemical bonding via a subsequent reaction. The B–H–B bond has three possibilities in subsequent reaction steps.

(1) The unsupported B–H–B bond is cleaved by a subsequent reaction. As described above, when $NH_2BH_3^-$ reacted with THF·BH_3 to form $NH_2BH_2(\mu\text{-}H)BH_3^-$, the unsupported B–H–B bond broke, resulting in the formation of the final products of the $(NH_2BH_2)_n$ polymer and BH_4^- anions.[14] In this reaction, the formation of the $(NH_2BH_2)_n$ precipitate and the stable BH_4^- anion provides the reaction driving force. Another example is the $B_2H_7^-$ anion formed by the reaction of BH_4^- with THF·BH_3: it can reversibly convert to THF·BH_3 and BH_4^- by cleaving the unsupported B–H–B bond (Figure S2). It is beleived that, compared with a bridge hydride, the coordinating solvents are better eletron donors and the solvent molecules can readily break the weak B–H–B bond to replace the bridge hydride from the B atom in the B–H–B bond.

(2) The unsupported B–H–B bond survives in non-coordinating solvents. The stability of the B–H–B bond depends on the countercation and the coordination ability of the solvents. Although LiB_2H_7 cannot be isolated from the reaction of $LiBH_4$ and THF·BH_3 in THF solution (Figure S2), the reaction of NR_4BH_4 (R = C_2H_5, C_4H_9) with B_2H_6 in CH_2Cl_2 solution afforded $NR_4B_2H_7$ which was isolated (eq 3):[15]

$$NR_4BH_4 + \frac{1}{2}B_2H_6 \rightarrow NR_4B_2H_7 \qquad (R = C_2H_5, C_4H_9) \tag{3}$$

This result indicates that $B_2H_7^-$ is only stable in noncoordinating solvents with an organic counter cations.

(3) The unsupported B−H−B bond survives in the final products with the cooperation of other chemical bonds. In the reaction of AB with THF·BH_3 in THF solution, the hydride in AB attacked the B in THF·BH_3 to substitute THF forming the AaDB intermediate, which is unstable and can only be observed in its ^{11}B NMR in the reaction solution.[11a] However, the subsequent molecular hydrogen elimination resulted in the formation of a stable four-membered ring compound (ADB), in which the formation of the B−NH_2−B bond stabilizes the B−H−B bond,[11b,c] as depicted in Scheme 3 and Scheme S1b.

Scheme 3. Formation of ADB by Reaction of NH_3BH_3 and THF·BH_3 in Which the Formation of the B−NH_2−B Bond Stabilizes the Formed B−H−B Bond

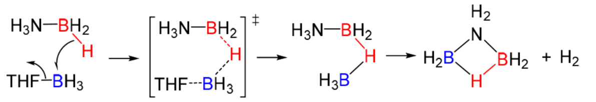

Another example is the dimerization of two BH_3 groups to form diborane in which one unsupported B−H−B bond formed first and the second B−H−B bond formed subsequently, resulting in a relatively stable B_2H_6 (Scheme S1a).

These reactions demonstrate that the nucleophilic substitution of the B−H bond can lead to a new B−H−B bond. However, whether the resulting B−H−B bond can survive in the final product depends on the reaction conditions[15] or if a subsequent reaction can take place to form a stable final product.[11b,c] This is probably why the nucleophilic substitution of the B−H bond has not attracted much attention, even though it has been known to occur for a long time.

Formation Mechanisms of Octahydrotriborate Anion. The formation mechanism of octahydrotriborate has been discussed previously, but it has not been fully understood.[1a,2k−o] On the basis of the nucleophilic properties of the B−H bond discussed above, we have elucidated the formation mechanisms of octahydrotriborate. Due to the better solubility of lithium borohydride in THF, we have chosen the reaction of $LiBH_4$ with THF·BH_3 for the mechanistic study. In this reaction, the BH_4^- anion acts as a nucleophilic reagent, using the B−H bond to attack the B in THF·BH_3 and substitute THF to give $B_2H_7^-$ by forming an unsupported B−H−B bond (Scheme 1B). The $B_2H_7^-$ product was clearly observed in solution on the basis of ^{11}B NMR, even though the product could not be isolated because of a reversible reaction (Figure S2). Envisioning that the resulting $B_2H_7^-$ anion may undergo a similar substitution reaction with a second THF·BH_3 to form a $H_3B(\mu\text{-H})BH_2(\mu\text{-H})BH_3$ anion ($B_3H_{10}^-$), we reacted $LiBH_4$ with 2 equiv of THF·BH_3. However, only the starting materials and the $B_2H_7^-$ signals were observed in the ^{11}B NMR at room temperature (Figure S3) or even at 50 °C (Figure 1a). But when the reaction mixture was refluxed, the $B_3H_8^-$ signal appeared (Figure 1b) and THF·BH_3 could be completely consumed after reflux for about 36 h (Figure 1e).

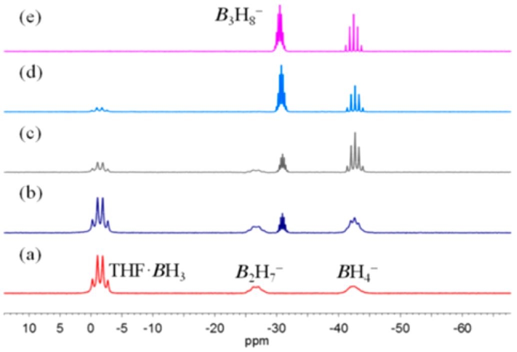

Figure 1. ^{11}B NMR spectra of $LiBH_4$ and THF·BH_3 in THF (a) at 50 °C for 12 h and under reflux condition for (b) 6 h, (c) 15 h, (d) 24 h, and (e) 36 h.

In order to gain more insights into the formation mechanism of $B_3H_8^-$, density functional theory (DFT) calculations were performed using the Gaussian 09 program.[16] The theoretical results are consistent with the experimental observations: BH_4^- reacts with the first THF·BH_3 to form $B_2H_7^-$ by attacking the B of THF·BH_3 with the B−H bond. The free energy barrier of the transition state TS1 is computed to be 15.8 kcal/mol in THF solvent (Table 1). Then, a terminal hydride of $B_2H_7^-$ further attacks the B in the second THF·BH_3 to replace THF to form $B_3H_{10}^-$ (Figure 2). This reaction requires a free energy of 10.3 kcal/mol, but the reverse energy barrier is much lower (2.4 kcal/mol, Figure 2).

Table 1. Calculated Electronic Energy (at 0 K), Enthalpy (at 298 K), and Free Energy (at 298 K) in kcal/mol

	Δ*E* (0 K)	Δ*H* (298 K)	Δ*G*/ΔG_{corr}[a] (298 K)
THF·BH_3 + BH_4^-	0	0	0
TS1	20.6	18.9	18.6/15.8
THF + $B_2H_7^-$	2.5	2.4	0.7
THF·BH_3 + $B_2H_7^-$	0	0	0
TS2	15.4	14.3	13.1/10.3
THF + $B_3H_{10}^-$	9.9	9.0	7.9
$B_3H_{10}^-$	0	0	0
TS3	5.9	4.8	6.0
B_2H_6 + BH_4^-	1.3	1.2	0.9
TS4	34.3	31.4	32.0
B_2H_5+$BH_3(H_2)$	33.5	31.8	31.4
TS5	42.4	38.1	36.6
$B_3H_8^-$ + H_2	−4.9	−6.1	−11.2
2THF·BH_3	0	0	0
TS1-1	13.9	14.7	15.5/12.7
THF·B_2H_6 + THF	5.0	8.9	10.1
THF·B_2H_6	0	0	0
TS2-1	3.1	4.8	5.1
B_2H_6 + THF	−6.7	−0.1	−2.0

[a] ΔG_{corr} = Δ*G* − 2.8 kcal/mol, based on free volume theory for bimolecular reactions in solution.

The DFT calculation further provides significant insight about how $B_3H_{10}^-$ converts to $B_3H_8^-$ by eliminating molecular hydrogen, which is important because no intermediates could be captured experimentally. First, we calculated the NPA charges and found that the charges of all the hydrogen atoms are negative (Figure 3a), implying that direct hydrogen release from $B_3H_{10}^-$ would be difficult. Interestingly, a transition state TS3 for the formation of B_2H_6 and BH_4^- was located with an energy barrier of only 6.0 kcal/mol (Figure 4). The natural population analysis (NPA) charges of the $B_2H_6\cdots BH_4^-$ complex showed that the bridge hydrogens are positively charged (0.11 and 0.19) and the hydrogens of BH_4^- are negatively charged (Figure 3b), suggesting the possibility of hydrogen elimination by the $H^{\delta+}\cdots H^{\delta-}$ interaction, a dihydrogen bond.[11d]

DOI: 10.1021/jacs.8b03785
J. Am. Chem. Soc. 2018, 140, 6718−6726

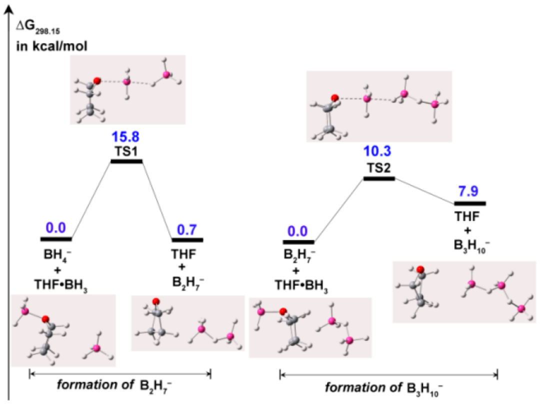

Figure 2. Energy profiles for the reactions from BH_4^- and THF·BH_3 to $B_3H_{10}^-$.

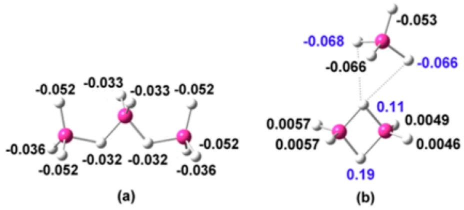

Figure 3. NPA charges of (a) $B_3H_{10}^-$ and (b) $B_2H_6\cdots BH_4^-$.

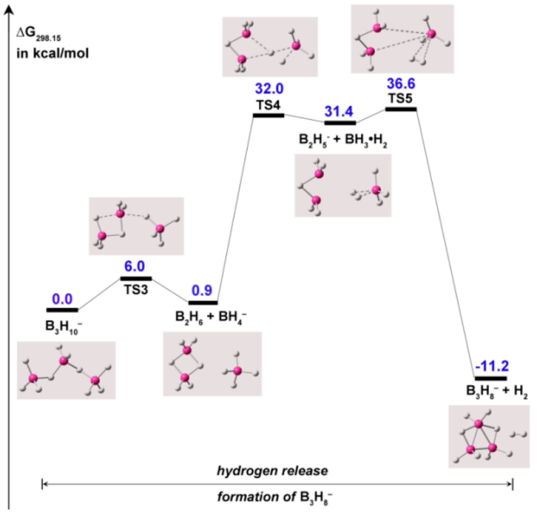

Figure 4. Energy profiles for the reaction from $B_3H_{10}^-$ to $B_3H_8^-$.

The $B_2H_5^-$ and $BH_3(H_2)$ intermediates were formed through TS4 with a calculated energy barrier of 31.1 kcal/mol in THF solvent. Then molecular hydrogen elimination (TS5) resulted in the formation of $B_3H_8^-$, which is exothermic by 11.2 kcal/mol (Figure 4).

According to the energy profiles of Figures 2 and 4, the B_2H_6 intermediate has two possible reactions: reacting with BH_4^- to reversibly re-form $B_3H_{10}^-$ and further to $B_2H_7^-$ (reaction 1) or reacting with BH_4^- to convert to $B_3H_8^-$ by releasing one H_2 (reaction 2). Furthermore, B_2H_6 could also react with the THF solvent to form THF·BH_3 as the reverse reactions shown in Figure 5 (reaction 3). Though the possible reactions 1 and 3 have relatively low energy barriers of 5.1 and 2.4 kcal/mol (TS3 and TS2, reverse reactions) and 7.1 and 2.6 kcal/mol (TS2-1 and TS1-1, reverse reactions) (Figure 5), respectively, a higher temperature would be required to form $B_3H_8^-$ via reaction 2.

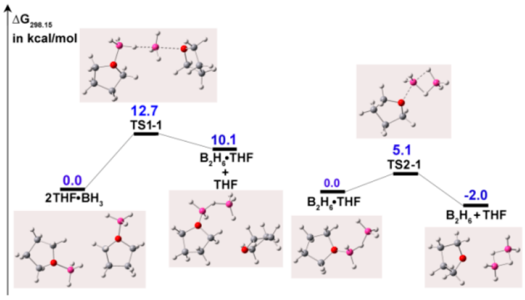

Figure 5. Formation mechanism of B_2H_6 from two THF·BH_3.

Once formed, the final product $B_3H_8^-$ is stable and cannot be reversibly converted to B_2H_6 and BH_4^- due to the high reverse-reaction energy barrier (47.8 kcal/mol). The escape of the resulting H_2 gas from the system would also make the reverse reaction impossible.

The experimental and computational results are fundamentally consistent with the proposed formation mechanism of $B_3H_8^-$. The low energy barriers of the two nucleophilic substitution reactions of BH_4^- and $B_2H_7^-$ with THF·BH_3 molecules to yield $B_3H_{10}^-$ (15.8 and 10.3 kcal/mol, respectively, in Table 1 and Figure 2) suggested that both reactions could occur at room temperature (Figure S2). Only the signal of $B_2H_7^-$ could be observed in the ^{11}B NMR due to the fact that the resulting $B_3H_{10}^-$ would be rapidly converted back to $B_2H_7^-$ with an energy barrier of only 2.4 kcal/mol (TS2, reverse reaction) or further converted to B_2H_6 and BH_4^- via TS3 with an energy barrier of only 6.0 kcal/mol. The calculated energy barrier of 31.1 kcal/mol (TS4) for the reaction of B_2H_6 and BH_4^- to produce $B_3H_8^-$ in THF supports the experimental observation that this reaction only occurred under reflux condition. Furthermore, the transformation from $B_3H_{10}^-$ to $B_3H_8^-$ is exothermic by 11.2 kcal/mol, so $B_3H_8^-$ is expected to be very stable once formed.

Observation of the B_2H_6 Intermediate and Its Roles in the Reactions To form $B_3H_8^-$. The B_2H_6 formed via TS3 seems to be a key intermediate in the proposed mechanism. Hence, it would be important to find out how B_2H_6 is formed and the roles it plays in the reactions. However, it is difficult to detect the formed B_2H_6 in THF solution because B_2H_6 would rapidly react with THF to produce the starting material THF·BH_3 (reaction 3). On the other hand, it is known that the BH_3 group exists as a B_2H_6 dimer rather than L·BH_3 in diethyl ether (Et_2O).[17] We also did experiment and found that the BH_3 group exists as the B_2H_6 dimer in dimethoxyethane (DME), albeit with a limited solubility (Figure S4).[11j] So we chose Et_2O to trap the resulting gases in the reaction of $LiBH_4$ with THF·BH_3. We indeed captured B_2H_6 and identified it by ^{11}B NMR (Figure S5).

In order to determine the roles of the B_2H_6 intermediate in the reactions, we used Et_2O and DME as solvents to investigate the reaction of B_2H_6 with $LiBH_4$ to gain further insight into the proposed mechanisms. In both Et_2O and DME solvents, we expect that the hydride of BH_4^- attacks the B in B_2H_6, breaking one of its H-bridge bond to form $B_3H_{10}^-$ by one step (Scheme 4). Even though the nascent $B_3H_{10}^-$ cannot be observed experimentally, its lower-barrier reverse reactions via TS2 (Figure 2) should be able to be observed.

Indeed, when an excess amount of B_2H_6 was bubbled into a DME solution of $LiBH_4$ at low temperature (−78 °C), the signals corresponding to the BH_4^- starting material and the

Scheme 4. Proposed Mechanisms of the Reaction between B_2H_6 with $LiBH_4$ in DME To Produce LiB_2H_7 and $LiBH_4$ or Produce LiB_3H_8 under Reflux

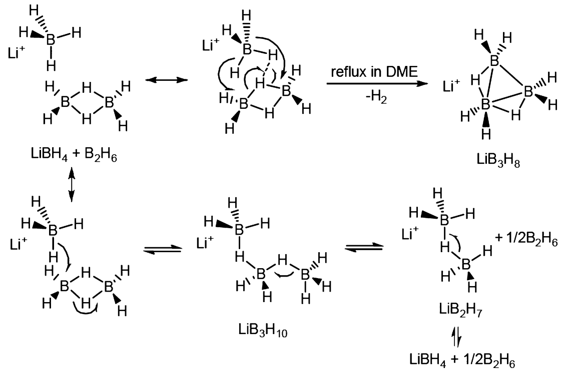

expected $B_2H_7^-$ product were clearly observed in ^{11}B NMR (Figure S6a). This observation confirmed that B_2H_6 reacted with BH_4^- at low temperature to form $B_3H_{10}^-$ via TS3 (the energy barrier of 5.1 kcal/mol, reverse reaction), which then form $B_2H_7^-$ facilely via TS2 (barrier of only 2.4 kcal/mol). The observation of the BH_4^- signal implies that the reaction could not be completed at low temperature. No B_2H_6 signal was observed, probably due to the limited solubility of B_2H_6 in DME at the low temperature. When the experiment was carried out at room temperature, only $B_2H_7^-$ signal was observed (Figure S6b), suggesting that BH_4^- can completely react with excessive B_2H_6 in DME at room temperature. Furthermore, when the B_2H_6 bubbling experiment was carried out under reflux condition, the $B_3H_8^-$ signal appeared (Figure S6c) and simultaneously a large amount of BH_4^- formed. This observation indicated that the reflux temperature of DME provides enough reaction driving force for the formation of $B_3H_8^-$ by crossing the high energy barrier of TS4 (31.1 kcal/mol). The large amount of BH_4^- is expected, due to the low energy barrier for the formation of BH_4^- via TS1 (reverse reaction).

Similar B_2H_6 bubbling experiment was also carried out in Et_2O with similar observations. Both $B_2H_7^-$ and BH_4^- signals were observed at low and room temperatures (Figures S7, S8a). However, when the B_2H_6 bubbling experiment was carried out under reflux, only a BH_4^-signal was observed in ^{11}B NMR without the $B_3H_8^-$ signal (Figure S8b). We think the low boiling point of Et_2O cannot drive the reaction to cross the high energy barrier of TS4 (31.1 kcal/mol). On the other hand, the formed $B_2H_7^-$ anion could convert to BH_4^- after cleaving BH_3 under reflux by crossing TS1 (reverse reaction, Figure 2). The cleaved BH_3 dimerized to B_2H_6, which escaped from the reaction mixture. Thus, only BH_4^- signal was observed under reflux (Scheme S2). These results confirmed the two possible reactions 1 and 2 of B_2H_6 and BH_4^- in the proposed mechanism.

Trapping B_2H_6 Formed from THF·BH_3. After finding the crucial roles of the B_2H_6 intermediate in the reactions to form $B_3H_8^-$, we further explored whether B_2H_6 could be formed by other pathways, other than from $B_3H_{10}^-$. The BH_3 group was known to exist as a B_2H_6 dimer in Et_2O, so it was used to trap the resulting gases when a THF·BH_3 solution (1 M) was refluxed without addition of $LiBH_4$ for 36 h. Indeed, we found that B_2H_6 and other unidentified boranes were formed (Figure S9). We were surprised that B_2H_6 could also be trapped in Et_2O when N_2 was simply bubbled through a THF·BH_3 solution (1 M) at room temperature (Figure S10).[18] Thus, the formed B_2H_6 in the proposed mechanism might be from the THF·BH_3 solution. With this consideration, the second possible pathway was proposed (Scheme 4) and the calculation results support the new proposed pathway for the formation of B_2H_6 (Figure 4).

In THF·BH_3 solution, the B−H bond in one THF·BH_3 molecule acts as a nucleophile to attack the B in another THF·BH_3 molecule to form THF·B_2H_6 (TS1-1, 12.7 kcal/mol) (Figure 5). Then, the terminal hydride of the BH_3 moiety in THFBH_2(μ-H)BH_3 attacked another B in the same intermediate to form B_2H_6 with THF leaving and ring closing (TS2-1, 5.1 kcal/mol) (Figure 5, Scheme S1). The resulting B_2H_6 can react with BH_4^- through reaction 1 or 2 as described above.

Isotopic experiment indicated that the deuteride/hydride exchange between THF·BD_3 and $LiBH_4$ occurred rapidly; thus the rate of the formation of $B_2H_7^-$ did not change obviously (Figure S11, Scheme S3). However, the rate of the formation of LiB_3H_8 is much slower, which revealed that the cleavage of the B−H bond to form H_2 is the rate-limiting step (Figure S12). This result is consistent with the proposed mechanisms.

The combination of experimental and computational studies indicated that B_2H_6 can be formed via both proposed pathways. The formation of B_2H_6 by the second pathway needed to cross the highest energy of 12.7 kcal/mol (TS1-1), but in the first one it is 15.8 kcal/mol (TS1). On considering the fact that $B_2H_7^-$ can be formed at both room and low (−78 °C) temperatures (Figure S13), the second proposed pathway seems to be more favorable. A previous report of the reaction between B_2H_6 and alkali metal borohydrides in ethers at 100 °C readily produced octahydrotriborate salts.[2k] Recent studies indicated that B_2H_6 produced in situ reacted with sodium borohydride to produce NaB_3H_8.[2l−o] A gas−solid reaction of B_2H_6 with $MgNiH_4$ was found to produce $Mg(B_3H_8)_2$. It is believed that the $Mg(BH_4)_2$ intermediate continually reacted with B_2H_6 to produce the final product.[1a] All of these experimental results seem to support the second pathway, but the first one cannot be ruled out.

The experimental and computational results discussed above suggested that the two proposed pathways from the starting reagents of THF·BH_3 and BH_4^- to the B_2H_6 + BH_4^- intermediates consist of a complicated set of reactions and reverse reactions that can be represented by a reaction circle at room temperature (Scheme S4). All the species in the circle, THF·BH_3 + BH_4^-, $B_2H_7^-$, $B_3H_{10}^-$, B_2H_6 + BH_4^-, and THF·BH_2(μ-H)BH_3, could be reversibly converted to its neighboring species at room temperature. The elimination of H_2 could not happen directly from $B_3H_{10}^-$ to produce $B_3H_8^-$. Only at reflux condition could the reaction of B_2H_6 with BH_4^- afford the $B_2H_5^-$ and $BH_3(H_2)$ intermediates, from which a H_2 elimination led to the formation of $B_3H_8^-$ (Scheme S4). This level of complexity underlies the reason why it has been difficult to understand the formation mechanisms of $B_3H_8^-$.

New Methods for the Syntheses of Lithium and Sodium Octahydrotriborate. The previously reported syntheses of the octahydrotriborate anion were all carried out by reacting boranes (diborane or THF·BH_3) with alkali metal amalgam or alkali metal dispersing in other media such as silica gel or inert salt or in the presence of other electron carriers (naphthalenide and tetraphenylborate).[2a−j] Moreover, in these reactions the final products are $B_3H_8^-$ and BH_4^- salts in 1:1 ratio (eq 1); i.e., at least a quarter of boranes did not convert to the expected product. There has been no report for preparation of octahydrotriborates by straightforwardly reacting borohydride with THF·BH_3. On the basis of the understanding of the nucleophilicity of the B−H bond and the formation mechanism of $B_3H_8^-$, we have developed a new and facile synthetic method for lithium and sodium salts of octahydrotriborate (eq 2). A mixture of $LiBH_4$ and THF·BH_3 in 1:2 ratio in THF solution was refluxed for 36 h. We observed that most of the starting materials were converted to $B_3H_8^-$, according to eq 2.

Only a small amount of $LiBH_4$ was left in the solution on the basis of the ^{11}B NMR (Figure 6a). After a small amount of water was added to consume the unreacted $LiBH_4$ (Figure 6b), the reaction mixture was filtered and the filtrate was then pumped under kinetic vacuum to produce an oily solid product, which was confirmed by ^{11}B and ^{1}H NMR (Figures S14 and S15) to be the desired $Li(THF)_{1.5}B_3H_8$ product with a purity of 95% in 41% isolated yield.

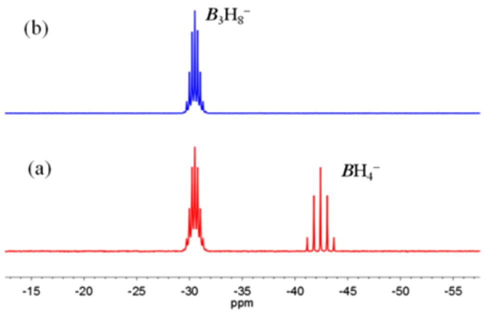

Figure 6. ^{11}B NMR spectra of the reaction solution of $LiBH_4$ and THF·BH_3 in THF refluxed for 36 h (a) and after addition of water (0.5 mL) into the reaction solution (b).

A small amount of the $LiBH_4$ reactant was always observed in the reaction solution, even if an excess amount of THF·BH_3 was used. This observation was mainly due to the fact that part of THF·BH_3 reactant was converted to B_2H_6 and other borane complexes (unidentified currently) when the THF·BH_3 solution was refluxed. The formed B_2H_6 was evaporated from the reacting system, as mentioned above (Figure S9), resulting in a net loss of the THF·BH_3 reactant. We found that the loss of THF·BH_3 via the release of B_2H_6 depended on the THF·BH_3 concentration. When a 1 M THF·BH_3 solution was refluxed for 36 h, about 32% of BH_3 was lost on the basis of the integrated values in ^{11}B NMR using NMe_3BH_3 as an internal standard (Figure S16). When a 0.5 M THF·BH_3 solution was refluxed for 40 h, about 25% of BH_3 was lost (Figure S17). When a 0.25 M THF·BH_3 solution was refluxed for 40 h, about 14% of BH_3 was lost (Figure S18). The inevitable loss of THF·BH_3 via B_2H_6 release under reflux was the reason why a small amount of unreacted $LiBH_4$ was always observed, even when an excess amount of THF·BH_3 was used.

The reactions of $LiBH_4$ with different concentrations of THF·BH_3 were carried out in order to examine the influence of the THF·BH_3 concentration on the yields and to optimize the reaction condition. As expected, a higher yield was obtained with a lower concentration of THF·BH_3. When a 0.5 and 0.25 M THF·BH_3 solution reacted with $LiBH_4$, the yields were 65% and 73%, respectively, based on the integrated values in ^{11}B NMR (NMR yield,[19] Figures S19 and S20), and the isolated yields were 54% and 66%, respectively. These are much higher than 55% (NMR yield) and 41% (isolated yield) of the reaction using 1 M THF·BH_3 solution (Figure S21). Furthermore, when a 20% excess amount of 0.5 or 0.25 M THF·BH_3 solution was used in the reaction, the yield was further increased to 79% and 81% (NMR yield) (Figures S22 and S23), and 69% and 73% (isolated yield) were calculated on the basis of $LiBH_4$.

In order to prevent the resulting B_2H_6 from escaping from the reaction system, we further carried out the reaction in an autoclave. When a 1 M THF·BH_3 solution reacted with $LiBH_4$ in the autoclave at 65 °C for 15 h, a NMR yield of 78.5% (Figure S24) and an isolated yield of 68% were achieved. Hence, we conclude that the reaction in autoclave is an efficient way for the preparation of lithium octahydrotriborate.

Slight decomposition of LiB_3H_8 to $LiBH_4$ was also observed in refluxing THF after 36 h (Figure S25). The unreacted or decomposed $LiBH_4$ could be easily removed by the addition of a small amount of water.

Sodium octahydrotriborate can be similarly prepared by using $NaBH_4$ and THF·BH_3, according to eq 2. A longer reaction time (66 h) was required because of poor solubility of $NaBH_4$ in THF. The purification procedure is similar to that of LiB_3H_8 (Figure S26). It is worthy to note that in this newly developed procedure, unsolvated NaB_3H_8 can be obtained simply by addition of only CH_2Cl_2 without further additoin of Et_2O as described in the literature.[2g] The purity of the final product is more than 95% on the basis of ^{11}B and ^{1}H NMR (Figures S27, S28) with a 43% isolated yield.

The isolated yield of NaB_3H_8 was incresed to 51% by using an autoclave at 65 °C for 24 h via the reaction of $NaBH_4$ with 1 M THF·BH_3, which is not a huge increase in comparison with the 43% yield for the reaction under reflux. The increase of the isolated yield is not as much as that in the $LiBH_4$ reaction. This could be attributed to the longer reaction time because of the limited solubility of $NaBH_4$ in THF, leading to more THF·BH_3 decomposition.

We should point out that the similar procedure cannot be used to prepare potassium octahydrotriborate probably due to the very low solubility of KBH_4 in THF (Figure S29).

■ CONCLUSIONS

In summary, the formation mechanisms of $B_3H_8^-$ from the direct reaction of BH_4^- and THF·BH_3 have been elucidated by the combination of experimental and computational studies based on the understanding of the nucleophilicity of the B−H bond. An intuitive mechanism for the formation of LiB_3H_8 was proposed. The nucleophilic substitution of the B−H bond in BH_4^- to THF in THF·BH_3 produced $B_2H_7^-$. The terminal B−H bond in $B_2H_7^-$ further substitutes THF in a second THF·BH_3 to produce $B_3H_{10}^-$. Theoretical calculations indicated that a H_2 molecule cannot be directly eliminated from $B_3H_{10}^-$ to form $B_3H_8^-$, but $B_3H_{10}^-$ could convert to B_2H_6 and BH_4^- and then to $B_2H_5^-$ and $BH_3(H_2)$ intermediates, from which the elimination of H_2 resulted in the final $B_3H_8^-$ product. The high calculated energy barrier of the $B_2H_6 + BH_4^- \rightarrow B_2H_5^- + BH_3(H_2)$ step (TS4 in Figure 4) is consistent with the experimental observation that this step can only take place under reflux. The $B_2H_7^-$ intermediate was observed in ^{11}B NMR, and the resulting B_2H_6 intermediate was captured. In another proposed mechanism, an initial reaction of two THF·BH_3 molecules produced B_2H_6, which further reacted with BH_4^- to form $B_2H_5^-$ + $BH_3(H_2)$ and then to $B_3H_8^-$. The conversion from B_2H_6 to $B_3H_8^-$ was confirmed experimentally. The fact that $B_2H_7^-$ can be formed not only at room temperature but also at low temperature (−78 °C) suggests that the second proposed pathway seems to be more favorable for the formation of $B_3H_8^-$, but the first one cannot be ruled out. The two proposed pathways consist of a reaction circle in which all species of THF·BH_3 + BH_4^-, $B_2H_7^-$, $B_3H_{10}^-$, B_2H_6 + BH_4^-, and THF·BH_2(μ-H)BH_3 could be reversibly converted to its neighboring species at room temperature. Only under reflux can the $B_3H_{10}^-$ intermediate be converted to the $B_3H_8^-$ via H_2 elimination. On the basis of the understanding of the formation mechanisms of $B_3H_8^-$, a facile method for the synthesis of MB_3H_8 (M = Li and Na) with high yields has been developed by the reactions of MBH_4 and THF·BH_3 under reflux. The synthetic method significantly simplifies the reaction procedures without using the highly toxic and reactive diborane, electron carriers, or other reaction media and allows convenient preparation of MB_3H_8 in large scales.

■ EXPERIMENTAL SECTION

General Remarks. All manipulations were carried out on a Schlenk line or in a glovebox filled with high-purity nitrogen. The ^{11}B NMR spectra were obtained at 128 or 193 MHz and externally referenced to BF_3·OEt_2 in C_6D_6 (δ = 0.00 ppm). The ^1H NMR and $^1H\{^{11}B\}$ spectra were obtained at 400 MHz.

Chemicals of $LiBH_4$, $NaBH_4$, KBH_4, NaH, $NaBD_4$, and I_2 were purchased from Sigma-Aldrich, and the NaH was washed with tetrahydrofuran (THF) and *n*-hexane. THF·BH_3, Me_3NBH_3, and NH_3BH_3 were purchased from United Boron (Zhengzhou) Energy Materials S&T LLC and used as received. $NaNH_2BH_3$ was prepared according to the literature.[20] B_2H_6 was prepared by the reaction of $NaBH_4$ with I_2 in DME (see Supporting Information).[21] THF, dimethoxyethane (DME), diethyl ether (Et_2O), *n*-hexane, and toluene were dried over sodium/benzophenone and freshly distilled prior to use. Dichloromethane was dried over calcium hydride.

Computational Details. All DFT calculations were performed using the Gaussian 09 program.[16] The geometries were optimized at M062X/6-311++G(d,p) level of theory, and single-point energy calculations in the THF solvent with the SMD approach[22] were carried out using the fully optimized geometries in vacuum. M062X functional was proved to be very accurate for reproducing thermodynamic data, barrier heights, and isomerization energies.[23] Vibrational frequencies were calculated at the same level to determine whether a species was an equilibrium structure or a transition state (TS). Occurence of imaginary vibrational frequencies would suggest the related species to be a TS. Natural population analysis (NPA) was used to evaluate atomic charges. Gibbs free energy (ΔG, kcal/mol at 298 K) barriers were computed to understand the reactions. For bimolecular reactions, it was difficult to accurately estimate activation entropies for the solution-based reactions. We corrected the activation Gibbs free energy ΔG (in kcal/mol) at 298 K using the free volume theory.[24] This provided a rate for a solution-based bimolecular reaction that was about 80 times faster than the corresponding reaction in the gas phase. This result suggested that the activation free energy for a solution reaction should be about 2.8 kcal/mol smaller than the value calculated in the gas phase. The Cartesian coordinates and vibrational frequencies of the studied model species are listed in the Supporting Information.

Reaction of $LiBH_4$ with THF·BH_3 at Room Temperature. In a drybox, $LiBH_4$ (0.11 g, 5 mmol) was put into a 50 mL flask which was connected to a Schlenk line and then 20 mL of THF·BH_3 (20 mmol) was condensed in to the flask at −78 °C. The reaction mixture was stirred for 20 h at room temperature. After the $LiBH_4$ reagent was completely consumed (Figure S2a), THF and excess THF·BH_3 were removed from the reaction solution under dynamic vacuum. The final residue sticky solid was identified as $LiBH_4$ by ^{11}B NMR (Figure S2b).

Reaction of $LiBH_4$ with THF·BH_3 at Low Temperature. In a drybox, $LiBH_4$ (0.11 g, 5 mmol) was put into a 25 mL flask which was connected to a Schlenk line and then 10 mL of THF·BH_3 (10 mL, 10 mmol) was condensed into the flask at −78 °C. The reaction mixture was stirred for 2 h at −78 °C, and then the mixture solution was transferred into a NMR tube which was kept in a −78 °C bath. The mixture was monitored by ^{11}B NMR at −88 °C (Figure S13).

Reaction of $NaNH_2BH_3$ with NH_3BH_3. $NaNH_2BH_3$ (0.53 g, 10 mmol) and NH_3BH_3 (0.31 g, 10 mmol) were placed in a 100 mL flask. About 30 mL of THF was condensed into the flask, and the reaction mixture was refluxed for 9 h. Then 30 mL of *n*-hexane was added into the solution and a white precipitate was formed. After filtration, THF and *n*-hexane were removed from the filtrate under dynamic vacuum to leave a white powder product $Na[BH_3NH_2BH_3]$ (0.25 g, 38%, Figure S1). ^{11}B NMR (128 MH_Z, THF-d_8): δ −19.9 (d, *J* = 90 Hz) ppm.

Reaction of B_2H_6 with $LiBH_4$ in DME. Lithium borohydride (0.11 g, 5 mmol) was added to a 25 mL flask and then 10 mL of DME was condensed into the flask at −78 °C. The prepared B_2H_6 by the reaction of $NaBH_4$ and I_2 (excess, about 10−15 mmol) with N_2 was bubbled into the reaction solution under stirring, and then the solution was monitored by ^{11}B NMR (Figure S6a). Similar precedures were carried out at both room temperature and under reflux. The resulting solutions were monitored by ^{11}B NMR (Figures S6b and S6c).

The reaction of B_2H_6 with $LiBH_4$ in Et_2O was similar to the reaction in DME. Detailed procedures are described in Supporting Information.

Stability of THF·BH_3. A sample of Me_3NBH_3 (0.73 g, 10 mmol) was added to a 50 mL flask, and then about 20 mL of 1 M THF·BH_3 was condensed into the flask. Then the solution was refluxed for 36 h and the evaporated gases were trapped by Et_2O (Figure S9) through the ice−water condenser. The mixture solution of Me_3NBH_3 and THF·BH_3 was determined by ^{11}B NMR before and after reflux (Figure S16). Similar procedures to examine the stability of 0.5 and 0.25 M THF·BH_3 under reflux are described in Supporting Information.

A sample of 1 M THF·BH_3 (20 mL, 20 mmol) solution was condensed into a 50 mL flask. At room temperature, N_2 was bubbled through the reaction solution at a flow rate of 5 mL min^{-1} for 6 h under constant stirring. And then the gases were trapped by Et_2O through ice−water condenser. The trapped Et_2O solution was examined by ^{11}B NMR (Figure S10).

Synthesis of $Li(THF)_{1.5}B_3H_8$. Lithium borohydride (0.44 g, 20 mmol) was added to a 100 mL flask, and then 1 M THF·BH_3 (40 mL, 40 mmol) was condensed into the flask. The reaction mixture was refluxed under stirring for 36 h. The formed gases were passed through tol-d_8, in which the formed H_2 was identifed (Figure S30). After reaction, a small amount of water (0.5 mL) was injected into the solution to destroy the residue $LiBH_4$. After filtration, THF was removed from the filtrate under dynamic vacuum to leave $Li(THF)_{1.5}B_3H_8$ as a clear oily product (NMR yield of about 55%, isolated yield of 1.27 g, 41% (Figures S14 and S15). ^{11}B NMR (128 MH_Z, D_2O): δ −31.2 (nonet, *J* = 33 Hz) ppm. ^{11}B NMR (128 MH_Z, CD_3CN): δ −30.8 (nonet, *J* = 33 Hz) ppm. ^1H NMR (400 MH_Z, D_2O): δ 3.77 (m, 4α-H of THF), 1.91 (m, 4β-H of THF), 0.30 (decet, *J* = 33 Hz, 8H of B_3H_8) ppm. $^1H\{^{11}B\}$ (400 MH_Z, D_2O): δ 3.78 (m, 4α-H of THF), 1.92 (m, 4β-H of THF), 0.3 (s, 8H of B_3H_8) ppm. ^1H NMR (400 MH_Z, CD_3CN): δ 3.65 (m, 4α-H of THF), 1.80 (m, 4β-H of THF), 0.13 (decet, *J* = 33 Hz, 8H of B_3H_8) ppm. $^1H\{^{11}B\}$ (400 MH_Z, CD_3CN): δ 3.65 (m, 4α-H of THF), 1.81 (m, 4β-H of THF), 0.13 (s, 8H of B_3H_8) ppm.

Similar procedures for synthesis of $Li(THF)_{1.5}B_3H_8$ by $LiBH_4$ with different concentrations of THF·BH_3 solutions are described in Supporting Information.

Synthesis of $Li(THF)_{1.5}B_3H_8$ in Autoclave. Lithium borohydride (0.22 g, 10 mmol) was added to a 50 mL autoclave, and then 1 M THF·BH_3 (20 mL, 20 mmol) was condensed into the autoclave. The reaction mixture was stirred for 15 h at 65 °C. Then THF and residue THF·BH_3 were removed from the reaction solution to leave a oily product. 20 mL of THF and water (0.1 mL) were injected into the oily product to remove the residue $LiBH_4$. After the formed precipitate was filtered, THF was removed from the filtrate under dynamic vacuum to leave $Li(THF)_{1.5}B_3H_8$ as a clear oily product (NMR yield of about 78.5%, isolated yield of 1.06 g, 68%, Figure S24).

Synthesis of Unsolvated NaB_3H_8. Sodium borohydride (0.76 g, 20 mmol) was added to a 100 mL flask, and then THF·BH_3 (40 mL, 40 mmol) was condensed into the flask. The reaction mixture was refluxed for 66 h under stirring. After filtration, water (0.05 mL) was injected into the solution to consume the soluble residue $NaBH_4$ in solution. The formed precipitate was filtered, and then THF was removed from the filtrate under dynamic vacuum to leave an oily product. The oily product was dissolved in CH_2Cl_2 and converted into suspension under stirring. After filtration, unsolvated NaB_3H_8 was obtained and dried under dynamic vacuum. Approximately 0.55 g of NaB_3H_8 was obtained with the 43% isolated yield (Figures S27 and S28; no NMR yield is available because $NaBH_4$ cannot be completely disolved in THF). ^{11}B NMR (128 MH$_Z$, CD_3CN): δ −30.0 (nonet, J = 33 Hz) ppm. ^1H NMR (400 MH$_Z$, CD_3CN): δ 0.14 (decet, J = 33 Hz) ppm.

Synthesis of Unsolvated NaB_3H_8 in Autoclave. Sodium borohydride (0.38 g, 10 mmol) was added to a 50 mL autoclave, and then 1 M THF·BH_3 (20 mL, 20 mmol) was injected into the autoclave. The reaction mixture was stirred for 24 h at 65 °C. After the insoluble $NaBH_4$ was filtered away, the THF and residue THF·BH_3 were removed from the reaction solution to leave a oily product. 20 mL of THF and water (0.05 mL) were injected into the oily product to destroy the soluble residue $NaBH_4$. After filtration, THF was removed from the filtrate under dynamic vacuum to leave a clear oily product. The oily product was dissolved in CH_2Cl_2 and converted into suspension under stirring. After filtration, unsolvated NaB_3H_8 was obtained and dried under dynamic vacuum (0.32 g, 51%).

Reaction of KBH_4 with THF·BH_3. Potassium borohydride (0.54 g, 10 mmol) was added to a flask, and then THF·BH_3 (20 mL, 20 mmol) was condensed into the flask. The reaction mixture was refluxed for 80 h under stirring, and a very small amount of $B_3H_8^-$ product was observed (Figure S29).

■ ASSOCIATED CONTENT

Ⓢ Supporting Information

The Supporting Information is available free of charge on the ACS Publications website at DOI: 10.1021/jacs.8b03785.

Details for experiments, characterizations, and computations (PDF)

■ AUTHOR INFORMATION

Corresponding Authors

*L.-S.W.: lai-sheng_wang@brown.edu
*J.Z.: jie.zhang@htu.edu.cn
*X.C.: xnchen@htu.edu.cn

ORCID

Nana Ma: 0000-0003-3225-9554
Lai-Sheng Wang: 0000-0003-1816-5738
Jie Zhang: 0000-0002-7693-6388
Xuenian Chen: 0000-0001-9029-1777

Author Contributions

$^\perp$X.-M.C. and N.M. contributed equally to this work.

Notes

The authors declare no competing financial interest.

■ ACKNOWLEDGMENTS

The authors are grateful for the financial support from the National Natural Science Foundation of China (Grants 21771057, 21571052, and 21603062) and the U.S. National Science Foundation (Grant DMR-1655066 to L.-S.W.). The authors thank Prof. Jun Li from Tsinghua University, Prof. Todd Marder from Universität Würzburg, Prof. Yanhui Guo from Fudan University, and Prof. Thomas Evans for valuable discussions.

■ REFERENCES

(1) (a) Huang, J.; Yan, Y.; Remhof, A.; Zhang, Y.; Rentsch, D.; Au, Y. S.; de Jongh, P. E.; Cuevas, F.; Ouyang, L.; Zhu, M.; Züttel, A. *Dalton Trans.* **2016**, *45*, 3687−3690. (b) Goedde, D. M.; Windler, G. K.; Girolami, G. S. *Inorg. Chem.* **2007**, *46*, 2814−2823. (c) Bykov, A. Yu.; Zhizhin, K. Yu.; Kuznetsov, N. T. *Russ. J. Inorg. Chem.* **2014**, *59*, 1539−1555.

(2) (a) Stock, A.; Pohland, E. *Ber. Dtsch. Chem. Ges. B* **1926**, *59*, 2210−2215. (b) Stock, A.; Laudenklos, H. B. *Z. Anorg. Allgem. Chem.* **1936**, *228*, 178−192. (c) Stock, A. *Hydrides of Boron and Silicon*; Cornell University, 1933; pp 58−58. (d) Hill, T. G.; Godfroid, R. A.; White, J. P.; Shore, S. G. *Inorg. Chem.* **1991**, *30*, 2952−2954. (e) Chen, W.; Wu, G.; He, T.; Li, Z.; Guo, Z.; Liu, H.; Huang, Z.; Chen, P. *Int. J. Hydrogen Energy* **2016**, *41*, 15471−15746. (f) Dunbar, A. C.; Macor, J. A.; Girolami, G. S. *Inorg. Chem.* **2014**, *53*, 822−826. (g) Huang, Z.; King, G.; Chen, X.; Hoy; Yisgedu, J. T. H.; Lingam, K.; Shore, S. G.; Woodward, P. M.; Zhao, J.-C. *Inorg. Chem.* **2010**, *49*, 8185−8187. (h) Fu, H.; Wang, X.; Shao, Y.; Chen, J.; Zhang, X.; Fu, H.; Zheng, J.; Li, X. *Int. J. Hydrogen Energy* **2016**, *41*, 384−391. (i) Zheng, X.; Yang, Y.; Zhao, F.; Fang, F.; Guo, Y. *Chem. Commun.* **2017**, *53*, 11083−11086. (j) Moury, R.; Gigante, A.; Hagemann, H. *Int. J. Hydrogen Energy* **2017**, *42*, 22417−22421. (k) Gaines, D. F.; Schaeffer, R.; Tebbe, F. *Inorg. Chem.* **1963**, *2*, 526−528. (l) Bykov, A. Yu.; Razgonyaeva, G. A.; Mal'tseva, N. N.; Zhizhin, K. Yu.; Kuznetsov, N. T. *Russ. J. Inorg. Chem.* **2012**, *57*, 471−473. (m) Myakishev, K. G.; Volkov, V. V. *Sib. Khim. Zh.* **1991**, *7*, 144. (n) Volkov, V. V.; Myakishev, K. G.; Gorbacheva, I. I. *Zh. Neorg. Khim.* **1989**, *34*, 1665−1668. (o) Volkov, V. V.; Gorbacheva, I. I.; Myakishev, K. G. *Zh. Neorg. Khim.* **1985**, *30*, 593−597.

(3) Kasper, J. S.; McCarty, L. V.; Newkirk, A. E. *J. Am. Chem. Soc.* **1949**, *71*, 2583−2583.

(4) Soldate, A. M. *J. Am. Chem. Soc.* **1947**, *69*, 987−988.

(5) (a) Buchi, G. D.; Ayer, E. *J. Am. Chem. Soc.* **1956**, *78*, 689−690. (b) Hough, W. V.; Edwards, L. J.; McElroy, A. D. *J. Am. Chem. Soc.* **1958**, *80*, 1828−1829.

(6) Olson, J. K.; Boldyrev, A. I. *Comput. Theor. Chem.* **2011**, *967*, 1−4.

(7) (a) Tanaka, N.; Shoji, Y.; Hashizume, D.; Sugimoto, M.; Fukushima, T. *Angew. Chem., Int. Ed.* **2017**, *56*, 5312−5316. (b) Braunschweig, H.; Chiu, C.-W.; Gamon, D.; Gruß, K.; Hörl, C.; Kupfer, T.; Radacki, K.; Wahler, J. *Eur. J. Inorg. Chem.* **2013**, *2013* (9), 1525−1530. (c) Romanescu, C.; Galeev, T. R.; Li, W. L.; Boldyrev, A. I.; Wang, L.-S. *Acc. Chem. Res.* **2013**, *46*, 350−358. (d) Zhai, H. J.; Chen, Q.; Bai, H.; Li, S. D.; Wang, L.-S. *Acc. Chem. Res.* **2014**, *47*, 2435−2445. (e) Kawai, S.; Saito, S.; Osumi, S.; Yamaguchi, S.; Foster, A. S.; Spijker, P.; Meyer, E. *Nat. Commun.* **2015**, *6*, 8098. (f) Kaiser, R. I.; Balucani, N. *Acc. Chem. Res.* **2017**, *50*, 1154−1162.

(8) (a) Brown, H. C.; Suzuki, A.; Miyaura, N.; Itoh, M.; Holland, G. W.; Negishi, E. *J. Am. Chem. Soc.* **1971**, *93*, 2792−2793. (b) Brown, H. C.; Gupta, S. K. *J. Am. Chem. Soc.* **1971**, *93*, 1816−1818. (c) Brown, H. C.; Gupta, S. K. *J. Am. Chem. Soc.* **1970**, *92*, 6983−6984. (d) Brown, H. C.; Kabalka, G. W. *J. Am. Chem. Soc.* **1970**, *92*, 714−716. (e) Xu, S.; Zhang, Y.; Li, B.; Liu, S.-Y. *J. Am. Chem. Soc.* **2016**, *138*, 14566−14569. (f) Yang, D.-T.; Mellerup, S. K.; Wang, X.; Lu, J.-S.; Wang, S. *Angew. Chem., Int. Ed.* **2015**, *54*, 5498−5501.

(9) Geier, S. J.; Vogels, C. M.; Westcott, S. A. In *Boron Reagents in Synthesis*; Coca, A., Ed.; ACS Symposium Series, Vol. 1236; American Chemical Society: Washington, DC, 2016; pp 209−225, DOI: 10.1021/bk-2016-1236.ch006.

(10) (a) Heuclin, H.; Ho, S.Y.-F.; Le Goff, X. F.; So, C.-W.; Mézailles, N. *J. Am. Chem. Soc.* **2013**, *135*, 8774−8777. (b) Borger, J. E.; Ehlers, A. W.; Lutz, M.; Slootweg, J. C.; Lammertsma, K. *Angew. Chem., Int. Ed.* **2016**, *55*, 613−617. (c) Wrackmeyer, B.; Klimkina, E. V.; Milius, W. *Eur. J. Inorg. Chem.* **2014**, *2014* (28), 4865−4876. (d) Chen, W.-C.; Lee, C.-Y.; Lin, B.-C.; Hsu, Y.-C.; Shen, J.-S.; Hsu, C.-P.; Yap, G. P. A.; Ong, T.-G. *J. Am. Chem. Soc.* **2014**, *136*, 914−917. (e) Celik, M. A.; Sure, R.; Klein, S.; Kinjo, R.; Bertrand, G.; Frenking, G. *Chem. - Eur. J.* **2012**, *18*, 5676−5692. (f) Jonas, V.; Frenking, G.; Reetz, M. T. *J. Am. Chem. Soc.* **1994**, *116*, 8741−8753.

(11) (a) Chen, X.; Bao, X.; Zhao, J.-C.; Shore, S. G. *J. Am. Chem. Soc.* **2011**, *133*, 14172−14175. (b) Chen, X.; Zhao, J.-C.; Shore, S. G. *J. Am. Chem. Soc.* **2010**, *132*, 10658−10659. (c) Li, H.; Ma, N.; Meng, W.; Gallucci, J.; Qiu, Y.; Li, S.; Zhao, Q.; Zhang, J.; Zhao, J.-C.; Chen,

X. *J. Am. Chem. Soc.* **2015**, *137*, 12406−12414. (d) Chen, X.; Zhao, J.-C.; Shore, S. G. *Acc. Chem. Res.* **2013**, *46*, 2666−2675. (e) Zhao, Q.; Li, J.; Hamilton, E. J. M.; Chen, X. *J. Organomet. Chem.* **2015**, *798*, 24−29. (f) Li, H.; Yang, Q.; Chen, X.; Shore, S. G. *J. Organomet. Chem.* **2014**, *751*, 60−66. (g) Shore, S. G.; Hall, C. L. *J. Am. Chem. Soc.* **1966**, *88*, 5346−5347. (h) Eastham, J. F. *J. Am. Chem. Soc.* **1967**, *89*, 2237−2238. (i) Shore, S. G.; Hall, C. L. *J. Am. Chem. Soc.* **1967**, *89*, 3947−3948. (j) Chen, X.; Bao, X.; Billet, B.; Shore, S. G.; Zhao, J.-C. *Chem. - Eur. J.* **2012**, *18*, 11994−11999.

(12) (a) Xu, Z.; Lin, Z. *Coord. Chem. Rev.* **1996**, *156*, 139−162. (b) Maseras, F.; Lledós, A.; Clot, E.; Eisenstein, O. *Chem. Rev.* **2000**, *100*, 601−636. (c) Esteruelas, M. A.; López, A. M.; Oliván, M. *Chem. Rev.* **2016**, *116*, 8770−8847. (d) Koehne, I.; Schmeier, T. J.; Bielinski, E. A.; Pan, C. J.; Lagaditis, P. O.; Bernskoetter, W. H.; Takase, M. K.; Würtele, C.; Hazari, N.; Schneider, S. *Inorg. Chem.* **2014**, *53*, 2133−2143. (e) Desrochers, P. J.; Sutton, C. A.; Abrams, M. L.; Ye, S.; Neese, F.; Telser, J.; Ozarowski, A.; Krzystek, J. *Inorg. Chem.* **2012**, *51*, 2793−2805. (f) Arliguie, T.; Belkhiri, L.; Bouaoud, S.-E.; Thuéry, P.; Villiers, C.; Boucekkine, A.; Ephritikhine, M. *Inorg. Chem.* **2009**, *48*, 221−230. (g) Demachy, I.; Esteruelas, M. A.; Jean, Y.; Lledós, A.; Maseras, F.; Oro, L. A.; Valero, C.; Volatron, F. *J. Am. Chem. Soc.* **1996**, *118*, 8388−8394. (h) Marks, S.; Heck, J. G.; Habicht, M. H.; Oña-Burgos, P.; Feldmann, C.; Roesky, P. W. *J. Am. Chem. Soc.* **2012**, *134*, 16983−16986. (i) Meyer, N.; Jenter, J.; Roesky, P. W.; Eickerling, G.; Scherer, W. *Chem. Commun.* **2009**, 4693−4695.

(13) Daly, S. R.; Bellott, B. J.; Kim, D. Y.; Girolami, G. S. *J. Am. Chem. Soc.* **2010**, *132*, 7254−7255.

(14) Chen, X.-M.; Li, H.; Yang, Q.-Y.; Wang, R.-R.; Hamilton, E. J. M.; Zhang, J.; Chen, X. *Eur. J. Inorg. Chem.* **2017**, *2017* (38−39), 4541−4545.

(15) (a) Shore, S. G.; Lawrence, S. H.; Watkins, R.; Bau, M. I. *J. Am. Chem. Soc.* **1982**, *104*, 7669−7670. (b) Hertz, R. K.; Johnson, H. D.; Shore, S. G. *Inorg. Chem.* **1973**, *12*, 1875−1877. (c) Evans, W. G.; Holloway, C. E.; Sukumarabandhu, K.; McDaniel, D. H. *Inorg. Chem.* **1968**, *7*, 1746−1748. (d) Brown, H. C.; Stehle, P. F.; Tierney, P. A. *J. Am. Chem. Soc.* **1957**, *79*, 2020−2021. (e) Brown, H. C.; Tierney, P. A. *J. Am. Chem. Soc.* **1958**, *80*, 1552−1558.

(16) Frisch, M. J.; Trucks, G. W.; Schlegel, H. B.; Scuseria, G. E.; Robb, M. A.; Cheeseman, J. R.; Scalmani, G.; Barone, V.; Mennucci, B.; Petersson, G. A.; Nakatsuji, H.; Caricato, M.; Li, X.; Hratchian, H. P.; Izmaylov, A. F.; Bloino, J.; Zheng, G.; Sonnenberg, J. L.; Hada, M.; Ehara, M.; Toyota, K.; Fukuda, R.; Hasegawa, J.; Ishida, M.; Nakajima, T.; Honda, Y.; Kitao, O.; Nakai, H.; Vreven, T.; Montgomery, J. A., Jr.; Peralta, J. E.; Ogliaro, F.; Bearpark, M.; Heyd, J. J.; Brothers, E.; Kudin, K. N.; Staroverov, V. N.; Kobayashi, R.; Normand, J.; Raghavachari, K.; Rendell, A.; Burant, J. C.; Iyengar, S. S.; Tomasi, J.; Cossi, M.; Rega, N.; Millam, J. M.; Klene, M.; Knox, J. E.; Cross, J. B.; Bakken, V.; Adamo, C.; Jaramillo, J.; Gomperts, R.; Stratmann, R. E.; Yazyev, O.; Austin, A. J.; Cammi, R.; Pomelli, C.; Ochterski, J. W.; Martin, R. L.; Morokuma, K.; Zakrzewski, V. G.; Voth, G. A.; Salvador, P.; Dannenberg, J. J.; Dapprich, S.; Daniels, A. D.; Farkas, O.; Foresman, J. B.; Ortiz, J. V.; Cioslowski, J.; Fox, D. J. *Gaussian 09*, revision D.01; Gaussian, Inc.: Wallingford, CT, 2009.

(17) Gaines, D. F. *Inorg. Chem.* **1963**, *2*, 523−526.

(18) Although an attempt to trap and detect the formed B_2H_6 by a similar experiment at low temperature is unsuccessful, it does not imply that B_2H_6 cannot be formed in the THF solution.

(19) The NMR yield was obtained from the integrated values in ^{11}B NMR. The calculation was based on the LiB_3H_8 product and the $LiBH_4$ starting material since part of THF·BH_3 would convert to B_2H_6 and other unidentified boranes, which escaped from the system. For example, in Figure S19, the NMR yield of LiB_3H_8 was $(1/3)/[(1/3) + 0.18] = 65\%$. The NMR yield might not be very accurate because the integral values were from different types of boron atoms, $B_3H_8^-$ or BH_4^-.

(20) Xiong, Z.; Yong, C. K.; Wu, G.; Chen, P.; Shaw, W.; Karkamkar, A.; Autrey, T.; Jones, M. O.; Johnson, S. R.; Edwards, P. P.; David, W. I. F. *Nat. Mater.* **2008**, *7*, 138−141.

(21) Narayana, C.; Periasamy, M. *J. Organomet. Chem.* **1987**, *323*, 145−147.

(22) Marenich, A. V.; Cramer, C. J.; Truhlar, D. G. *J. Phys. Chem. B* **2009**, *113*, 6378−6396.

(23) (a) Zhao, Y.; Truhlar, D. G. *J. Phys. Chem. A* **2006**, *110*, 5121−5129. (b) Zhao, Y.; Truhlar, D. G. *Theor. Chem. Acc.* **2008**, *120*, 215−241.

(24) (a) Liu, Q.; Lan, Y.; Liu, J.; Li, G.; Wu, Y.-D.; Lei, A. *J. Am. Chem. Soc.* **2009**, *131*, 10201−10210. (b) Li, Z.; Fu, Y.; Guo, Q.-X.; Liu, L. *Organometallics* **2008**, *27*, 4043−4049.